High-Resolution STM Studies of Terephthalic Acid Molecules on Rutile TiO2(110)-(1 x 1) Surfaces

ARTICLE *in* THE JOURNAL OF PHYSICAL CHEMISTRY C · MAY 2009

Impact Factor: 4.77 · DOI: 10.1021/jp901184t

6 AUTHORS, INCLUDING:

Szymon Godlewski
Jagiellonian University
37 PUBLICATIONS **262** CITATIONS

SEE PROFILE

Janusz Budzioch
Janusz Budzioch MeasLine
22 PUBLICATIONS **202** CITATIONS

SEE PROFILE

High-Resolution STM Studies of Terephthalic Acid Molecules on Rutile TiO_2(110)-(1 × 1) Surfaces

Jakub S. Prauzner-Bechcicki,* Szymon Godlewski, Antoni Tekiel,† Piotr Cyganik, Janusz Budzioch, and Marek Szymonski

Research Centre for Nanometer-scale Science and Advanced Materials (NANOSAM), Faculty of Physics, Astronomy and Applied Computer Science, Jagiellonian University, Reymonta 4, 30-059, Krakow, Poland

Received: February 9, 2009; Revised Manuscript Received: March 20, 2009

The structure of terephthalic acid (TPA) molecules adsorbed on rutile TiO_2(110)-(1 × 1) has been investigated by scanning tunneling microscopy (STM). Molecularly resolved STM images show formation of monolayer with the tendency of TPA molecules to form dimer rows along the [001] substrate direction. The ability to image functional groups by the STM tip, and single molecule diffusion are demonstrated. The quality and stability of the monolayer are tested, including the resistance against air exposure. On the basis of results obtained, the model of TPA adsorption on the rutile TiO_2(110)-(1 × 1) is proposed.

I. Introduction

The surface of titanium dioxide is the most often studied metal oxide surface, which is also concerned as a model system for transition metal oxides.[1] The interest in titanium dioxide is mainly driven by its diverse applications including catalysis,[2−5] coating materials,[6−8] and sensor production[9−12] to name just a few. Considering this wide range of applications, the adsorption of organic molecules is certainly one of the most appealing directions in the surface science of TiO_2. Although metal oxides provide anisotropic surfaces and specific adsorption sites that would facilitate growth of well-ordered monolayers, the chemical functionalization of these surfaces by organic molecules is still in its preliminary stage.[1,13−20] In this contribution, we focus on scanning tunneling microscopy (STM) measurements of 1,4-benzenedicarboxylic acid (terephthalic acid, TPA) monolayers adsorbed on the rutile TiO_2(110)-(1 × 1) surface.

Our interest in studying adsorption of TPA is driven by the fact that TPA molecules are used in some of metal-organic frameworks (MOFs).[21] MOFs form a relatively new class of porous materials which consist of metal ions linked by specific organic molecules like the TPA. Due to their potential application in gas storage, molecular separation, and heterogeneous catalysis MOFs attract growing attention. Although MOFs are usually produced in the form of a powder, it was demonstrated recently that thin films of this material can be very selectively grown on surfaces functionalized by monolayers of organic molecules which mimic the functionality of organic linkers used for MOFs synthesis.[22−24] Formation of MOF thin films on desired substrates, called SURMOFs,[25] clearly opens up new opportunities for MOFs application, e.g., in design of sensors, as it was demonstrated very recently.[26] Along this line of research, formation of well-defined and stable TPA monolayers on the TiO_2 surface would enable later research on SURMOFs formation on this substrate, and at the same time, possibility of merging these two important classes of materials. For example, joining in one composite device the catalytic properties of the substrate with extraordinary storage capacity of MOFs for accumulation of products of catalytic reactions could be very advantageous. It is also worth mentioning that in contrast to previous studies on SURMOFs growth, formation of stable TPA monolayers on TiO_2 allows studying direct application of MOFs constituencies for initiating SURMOFs.

In our previous work,[20] we have reported on the first results of combined STM and non-contact atomic force microscopy (nc-AFM) measurements of TPA molecules adsorbed on the rutile TiO_2(110)-(1 × 1) surface. It was concluded that TPA molecules form a monolayer of upright standing molecules that supposedly expose one of their carboxyl groups to the vacuum interface. Here, we extended previous measurements by further STM studies addressing details of the film structure, defects formation and stability of TPA molecules on the rutile TiO_2(110)-(1 × 1) surface.

II. Experimental Section

The experiments were carried out in a multichamber ultrahigh vacuum (UHV) system, which consisted of a microscope, preparation, surface analysis, and radial distribution chambers. The base pressure in the microscope chamber, equipped with Omicron variable temperature scanning probe microscope (VT STM/AFM), was 4×10^{-11} mbar. In the remaining chambers of the UHV system, base pressure was in the low 10^{-10} mbar range. The preparation chamber was supplied with a noble gas ion gun, effusion cells, an infrared pyrometer, and a quartz microbalance thickness monitor. The surface analysis chamber was equipped with a low energy electron diffraction (LEED) system. The TiO_2(110) wafers (MaTecK GmbH) were mounted on sample holders with a silicon wafer as a resistive heater. The TiO_2 samples were first annealed for 6 h at 800 K, and subsequently subjected to repetitive cycles of 1 keV Ar^+ sputtering for 15 min and annealing at 960 K for 15 min until clean surface was reached. The annealing temperature was controlled by the infrared pyrometer. The quality of the obtained TiO_2(110)-(1 × 1) surface was monitored by STM and LEED measurements. The TPA molecules were evaporated at about 370 K from a Knudsen cell on the TiO_2(110) surface kept at room temperature. Pressure in the preparation chamber during TPA deposition was 9×10^{-10} mbar. Prior to the evaporation

* To whom correspondence should be addressed: E-mail: jakub.prauzner-bechcicki@uj.edu.pl.

† Present address: Department of Physics, McGill University, 3600 University Street, Montreal QC, H3A 2T8, Canada.

10.1021/jp901184t CCC: $40.75
Published on Web 04/30/2009

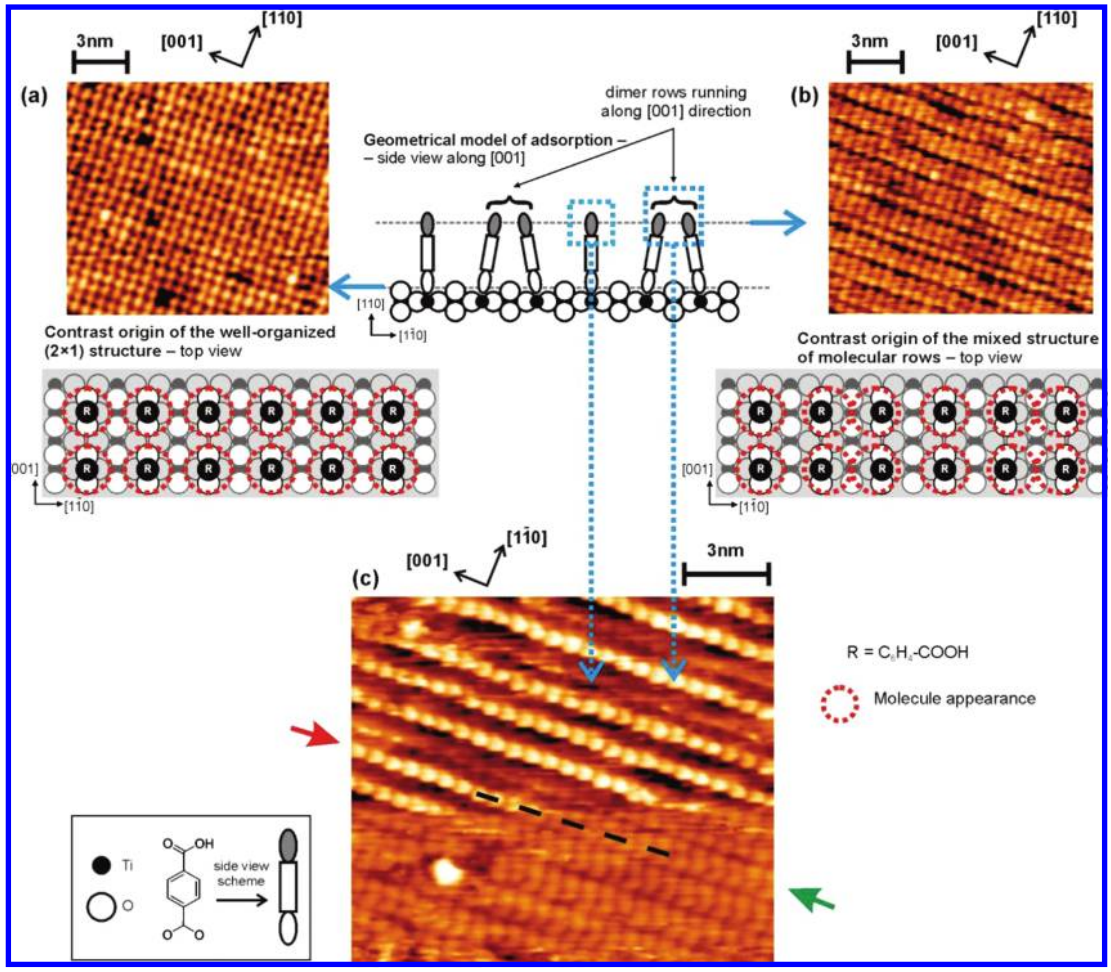

Figure 1. Images (a), (b), and (c) show different STM contrasts obtained at the same scanning parameters ($I = 2$ pA, $U = 1.8-2.0$ V) for the same sample of TPA/TiO_2(110). The cartoon located in the central part of the figure schematically shows the side view of the TPA monolayer. Blue arrows pointing images (a), (b), and (c) in this cartoon schematically show which part of the monolayer is presumably visualized by the given STM scan. The top view appearance of the monolayer in STM scans shown in (a) and (b) is schematically presented in cartoons displayed below respective image. Arrows on sides of image (c) point to rows of bright spots (red arrow) and S-shaped structures (green arrow), respectively (see text for details).

procedure, terephthalic acid powder (Fluka, ≥ 99% purity) was outgassed in vacuum. The STM imaging was carried out in a constant current mode at positive bias voltages, i.e., empty-states imaging, with etched tungsten tips used as probes. The image processing and analysis was done using WSxM 4.0 software.[27]

III. Results and Discussion

Structure of the Monolayer. Former studies on room temperature adsorption of monocarboxylic acids, such as formic, acetic, and trimethylacetic acids,[1,16] as well as, larger, aromatic monocarboxylic acids, such as benzoic and isonicotinic acids[13−15] demonstrated that carboxylic acids follow a dissociative adsorption path on the rutile TiO_2(110)-(1 × 1) surface. The adsorption process involves dissociation of the carboxyl group that gives carboxylate and hydrogen. In the following step, the negatively charged carboxylate is bounded in a bridge form with the O−C−O plane aligned in the [001] surface direction on a pair of 5-fold coordinated Ti atoms, and thus, occupies two surface lattice unit cells. The remaining hydrogen atom is presumably bounded to one or two surface oxygen atoms, forming −OH group or bridging two oxygen atoms, respectively. Lyubinetsky et al. suggested that presence of such −OH residues or bridging −H atoms might play a role in stabilizing the overlayer of trimethylacetic acid on the TiO_2(110) surface.[28]

Since the primary motivation of our research is well-defined, functionalization of the TiO_2(110) surface by TPA molecules to enable later growth of MOFs, we have focused our experiments on studying deposition conditions, which allow a full monolayer coverage. The high-resolution STM data presented in Figure 1 show densely packed structure of TPA molecules obtained at the full monolayer coverage (1 ML). Importantly, further increase of deposition time does not result in observation of second or higher order molecular layers, thus suggesting that adsorption of the TPA on the TiO_2(110)-(1 × 1) surface at room temperature is a self-limiting process, up to 1 ML coverage. Four different contrasts observed in our STM data are documented in Figure 1. Whereas the two first types of contrast depicted in Figure 1, parts a and b, we have already reported,[20] the other two contrasts shown in Figure 1c, have not been identified in our previous experiments. We have observed random, reversible switching between these four STM contrasts during data acquisition, which we attribute to a change of the STM tip termination. Several possibilities of a tip modification leading to the observed changes of the STM contrast can be considered including: (1) adsorption of a TPA molecule, (2) its further reorientation, or (3) transfer of the proton that comes from dissociation of TPA molecules and is supposedly adsorbed on the surface. Each of such changes of the STM tip apex may easily take place several times while scanning the monolayer

of TPA molecules on TiO_2(110) surface leading to reoccurrence of a given contrast. The more strict identification of the tip modification responsible for a given STM contrast requires a theoretical modeling which has not been done so far.

In Figure 1a, a regular (2 × 1) pattern is clearly visible. This structure is long-ranged, as it is documented by the 50 × 50 nm scans, which will be analyzed later on. Assuming that each bright spot in Figure 1a corresponds to one molecule, we obtain a packing density corresponding to one TPA molecule per two TiO_2(110)-(1 × 1) substrate unit cells, i.e., 38 Å^2 per molecule (2.61 × 10^{14} molecules/cm^2). These results indicate an upright orientation of the TPA molecules considering a previous study[15] for shorter molecules of isonicotinic acid on the TiO_2(110)-(1 × 1) substrate, where combined STM and angle-dependent X-ray absorption spectroscopy data demonstrated upright orientation of these molecules adsorbed in the similar (2 × 1) pattern. We attribute the observed (2 × 1) pattern to the adsorption sites of the TPA molecules, i.e., deeper lying electronic structures since it was not observed in the corresponding nc-AFM measurements reported in our previous paper.[20] The other common STM contrast, shown in Figure 1b, is the monomer−dimer motif which has been also observed in our previous nc-AFM measurements,[20] and therefore, we attribute it to the higher lying electronic structures. In this pattern, molecular rows are aligned along the [001] substrate direction. As documented by the data, monomer rows frequently evolve into dimer rows and vice versa.

The additional piece of information, regarding formation of this monomer−dimer pattern, can be found in the two other much less frequently observed STM contrasts visible in the upper and lower parts of the single STM image shown in Figure 1c. Whereas the upper part of this image exhibits bright spots forming rows along the [001] substrate direction (marked by the red arrow in Figure 1c), the lower part reveals dark lines separating rows of S-shaped structures (marked by the green arrow in Figure 1c). When comparing the position of the rows of bright spots in the upper part of Figure 1c with the rows of S-shaped structures in the lower part of this image, it becomes clear that the rows of bright features correspond to the enhanced contrast from the middle part of TPA dimer rows, i.e., S-shaped structures (compare dashed line in Figure 1c). Such a transition of the row of bright spots of the enhanced contrast into the middle part of the dimer rows was repeatedly observed. Therefore, we suppose that this enhanced contrast originates from the spontaneous tip apex modification by either an adsorbed TPA molecule or proton transfer, which enables recognition of the −COOH groups in a monolayer. The recognition of the functional −OH and −COOH groups via deliberate chemical modification of the STM tip with thiol self-assembled monolayers (SAMs) has been demonstrated by Ito et al. for the flat-laying physisorbed monolayers of 1-octadecanol and 1-octadecanoic acid on HOPG.[29] It has been suggested in this work that the contrast enhancement on hydroxyl or carboxyl groups originates from the hydrogen bond interaction between the functional groups of the tip and the sample. Such a hydrogen bond based contrast enhancement effect was also observed for polymer-modified tips.[30] For the TPA monolayer, observed contrast enhancement probably comes from the adsorption of a TPA molecule (or molecules) on the tip and formation of the hydrogen bond between the decorated tip and the molecules in the monolayer. Interestingly, the enhancement of the contrast is observed only for TPA molecules in dimer rows. The origin of this drastic difference in the visualization of the upright standing molecules arranged in dimer and monomer rows is not clear at the moment. However, it should be noted that in the previous experiments by Ito et al.[29] the drastic contrast enhancement was observed in the monolayers of physisorbed molecules where two neighboring −COOH or −OH groups were in contact (the molecules of 1-octadecanol or 1-octadecanoic acid on HOPG were physisorbed flat lying in the head-to-head configuration). Therefore, we suppose that higher contrast of the TPA molecules in the dimer configuration may result from their inclination, which enables contact between neighboring −COOH residues as it was observed in previous experiments by Ito et al. The other possibility for the STM contrast modification, which enables high chemical sensitivity, is by proton transfer to the tip apex, as proposed in the previous high-resolution STM studies of the pristine TiO_2 (110) surface.[31]

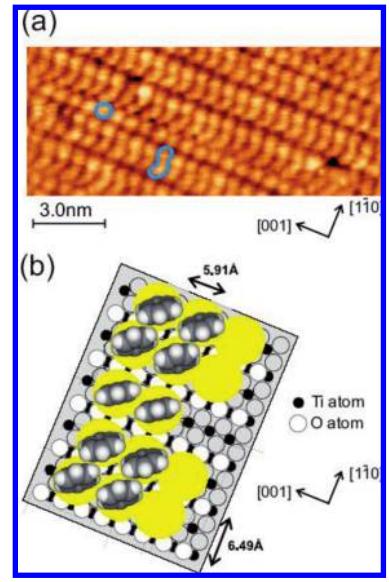

Figure 2. In (a) STM image (2pA, 2V) exhibiting rows of dimers and monomers on the TPA/TiO_2(110) sample. The round shape and S-shape characteristic for monomer and dimer rows, respectively, are marked in blue. The cartoon in (b) schematically shows possible tilting and rotating of the TPA phenyl rings associated with the dimer formation. For simplicity, only phenyl rings associated with the TPA molecules are shown in this cartoon. The STM contrast visible in (a) is schematically marked in (b) by yellow circles. The possible rotation by 25° of the TPA phenyl rings with respect to the O−C−O plane of the carboxyl group through which TPA binds to the substrate along the [001] substrate direction has been adopted from ref 32.

Another type of contrast visible in the lower part of Figure 1c is presented in more details in Figure 2a. In this STM image, TPA molecules in monomer rows are round shaped, similar to that observed for the data presented in Figure 1, parts a and b. In contrast, dimer rows are formed by the S-shaped structures with more elongated shape of the TPA molecules (see blue markers in Figure 2a). We suppose that these differences reflect inclination of the TPA molecules in dimer rows and possible rotation of the phenyl ring (see cartoon in Figure 2b). The possible rotation of the phenyl ring with respect to the O−C−O plane of the carboxyl group through which the molecule binds to the substrate is supported by the very recent theoretical calculations for the TPA molecules on Cu(110) substrate.[32]

Summarizing obtained results, we can propose a model of the TPA adsorption on the TiO_2(110)-(1 × 1) substrate, which is schematically depicted in Figure 1. The basic ingredients of this model are as follows: (i) molecules bind to the surface in a bidentate fashion on the two 5-fold coordinated Ti atoms, (ii) form rows along the [001] direction, (iii) are oriented upward

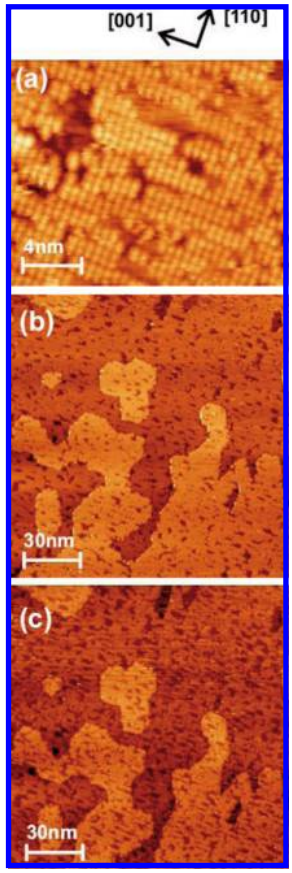

Figure 3. In (a) high-resolution STM image obtained for TPA/TiO_2(110) sample exhibiting 0.6 ML coverage (measured from STM images with use of WSxM 4.0 program [ref 27]) dimer pattern clearly visible in selected areas of the image. In (b) and (c) two consecutive STM images taken at the same location of the TPA/TiO_2(110) sample show STM induced reduction of the TPA coverage from 0.7 ML in (b) to 0.5 ML in (c). STM parameters: (a) $I = 2$ pA and $U = 2.0$ V, (b) $I = 20$ pA, $U = 2$V, (c) $I = 20$ pA, and $U = 2$V.

with −COOH group exposed to the vacuum interface, and (iv) incline and rotate toward each other to form dimers.

Defects Formation. Before discussing defects which are inherently present in the TPA monolayer, it is crucial to consider the influence of the STM imaging on the film stability. The data presented in Figures 1 and 2 have been obtained at the extremely low current set point of 2 pA, and relatively high bias voltage of 1.8−2.0 V. Generally, our experiments show that even for the STM imaging with 2 orders of magnitude higher current set point (keeping the same bias voltage), no systematic modification of the TPA film structure could be observed. This statement is, however, true only for the TPA coverage close to a complete monolayer. As it is exemplified by the data obtained for the TPA film corresponding to ∼0.6 ML coverage (coverage measured from the respective STM images with use of WSxM 4.0 program [ref 27]), the nondestructive high-resolution imaging of this sample could be performed at 2 pA current set point and 2 V bias voltage (Figure 3a), i.e., at extremely high impedance conditions. In contrast, the STM imaging of such low-coverage TPA samples at the current set point increased up to only 20 pA (keeping the same bias voltage) results in well visible TPA film modification. This observation is documented by the data shown in Figure 3, parts b and c, where two consecutive scans reveal STM-tip induced increase of dark patches in Figure 3, parts b and c, which correspond to regions free from TPA molecules. The more detailed analysis of these data show that single STM scan, at this imaging conditions, results in a decrease of the TPA coverage from the initial ∼0.7 down to ∼0.5 ML.

Three important conclusions can be drawn from the data shown in Figure 3. First, it is clear that nondestructive STM imaging of TPA films at the submonolayer coverage requires extremely high impedance conditions; otherwise, the interpretation of the obtained results may lead to severe problems. Second, the fact that the characteristic dimer packing motive of TPA molecules reported above for the full monolayer coverage is also present even at a much earlier stage of the film formation, i.e., at coverage of only 0.6 ML (see high-resolution data in Figure 3a), suggest rather important contribution of dimerization to the overall energetics of the TPA film formation on the TiO_2 (110) substrate. Finally, the very high sensitivity of the TPA film to the STM imaging only at low coverage, with at the same time unchanged TPA packing structure between a monolayer and submonolayer coverage, and film destruction starting from edges of TPA islands indicate that contribution of the intermolecular interactions to the overall energetics of the film is significant. This conclusion is also supported by recent theoretical calculations[33] performed for an individual TPA molecule on the TiO_2(110) surface which show TPA adsorption in flat laying geometry, and thus, indicate that formation of standing up (2×1) structure observed in our studies is driven by intermolecular interactions. Importantly, both later conclusions imply that dimerization process is related to the optimization of the intermolecular interaction, as it is assumed in the model proposed in Figure 1, rather than being an effect of the molecule−substrate binding geometry.

The basic defects that are observed for the noninvasive imaging conditions of the TPA monolayer are missing molecules. The identification of these defects depends on the termination of the STM tip. In particularly, the two basic STM contrasts reported in Figure 1, parts a and b, exhibit a different appearance of these defects. Figure 4 shows the same area of the TPA monolayer, which was imaged several times and due to a spontaneous tip change the two types of the STM contrasts of the same surface area were recorded (at the same values of the current set point and bias voltage). The contrast type shown in Figure 4, parts a and c, which reveals the (2×1) structure, exhibits pronounced black patches in some sample areas. One might interpret these depressions as real changes in the sample topography and thus missing molecules. However, the contrast type shown in Figure 4, parts b and d, which enables visualization of dimer rows, reveals that these black patches can correspond to both molecular vacancies (see white dotted circles in Figure 4, parts c and d) and still adsorbed molecules (see yellow dashed ellipses in Figure 4, parts c and d). It should be noted at this point that the image shown in Figure 4, parts b and d, has been acquired after collecting the image shown in Figure 4, parts a and c, and therefore the misinterpretation originating from tip-induced damage of the sample can be excluded. Nevertheless, we suppose that in the case of a defected layer, the scanning tip can have some influence on its appearance, e.g., it can smear the molecules at the edge of the uncovered area and slope them into it without removing them from the surface. Thus, some regions without molecules appear disordered and blurred in Figure 4, parts b and d (compare defects marked by black ellipses in Figure 4, parts a and b). Contrary to the previous case, some of the black patches present in Figure 4, parts a and c do not correspond to a disordered contrast in Figure 4, parts b and d (compare defects marked by yellow ellipses in Figure 4, parts c and d). Interestingly, in those regions, the molecules still build well-defined monomers or

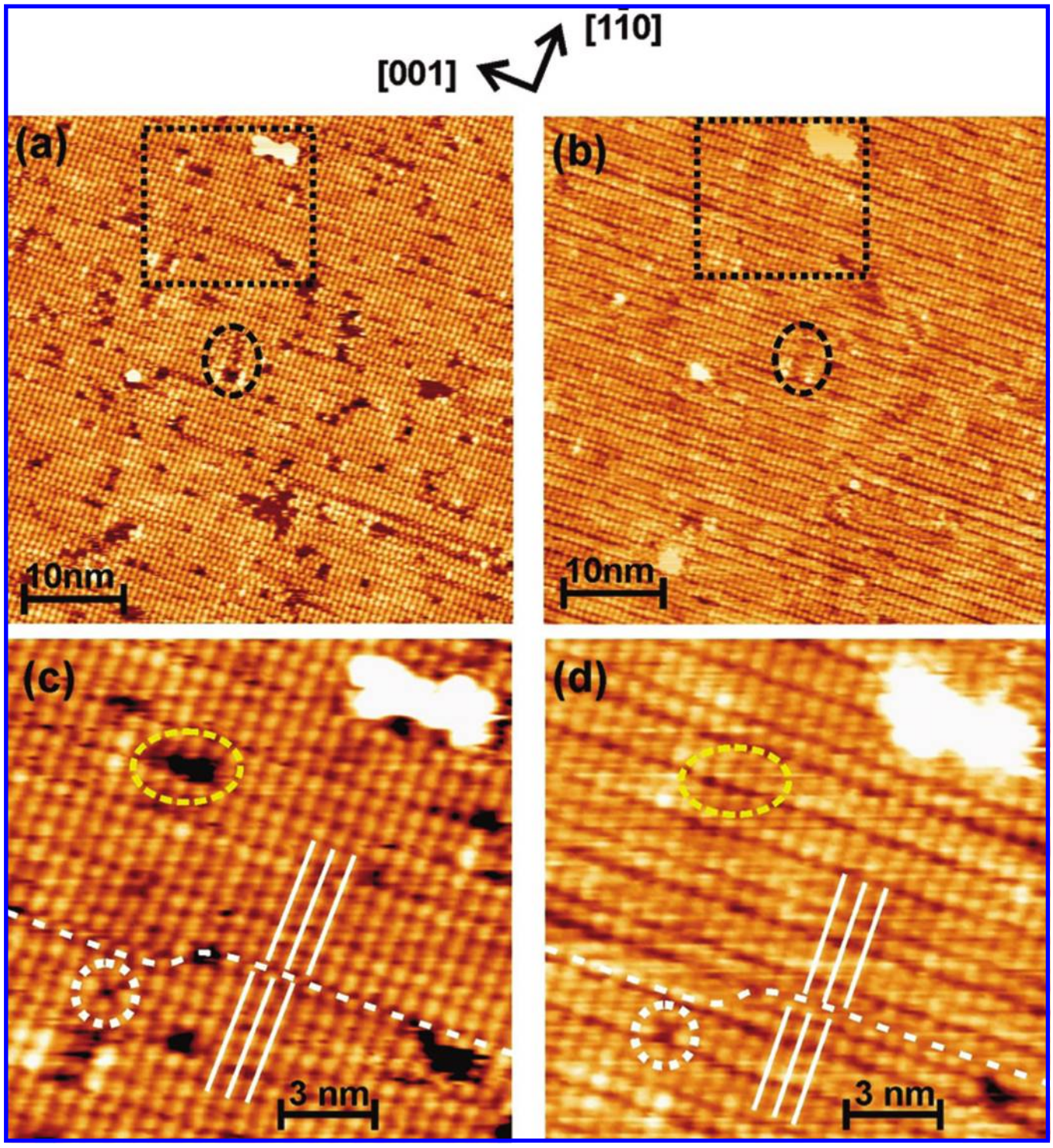

Figure 4. In (a) and (b); two STM images taken at the same location of the TPA/TiO_2(110) sample. Black rectangles marked in (a) and (b) correspond to the magnified areas shown in (c) and (d), respectively. White dotted loops and dotted lines in (c) and (d) mark single molecule vacancy and translational domain boundary (see white lines, which mark molecular rows), respectively. Dashed ellipses (black and yellow) mark different appearance of defects (see text for details). All images where acquired with the same imaging parameters ($I = 2$ pA, $U = 2.0$ V). Image in (a) was taken before image in (b).

dimers. We suppose that within these black patches, the TPA molecules are adsorbed in a different way in comparison to the majority of TPA molecules bounded in a bridge form over two Ti surface atoms. Presumably, this might be caused by the presence of surface defects or complex intermolecular interactions. Although a molecule adsorbs differently, e.g., binding to a single Ti atom as monodentate or bidentate, it still may adsorb in an upright orientation, especially at a monolayer coverage. This scenario allows for the creation of well-defined monomer and dimer rows but with locally perturbed adsorption geometry, which can lead to a different appearance of the imperfect region only in one of the discussed types of STM contrasts.

Another type of defects in the TPA film, marked by white dashed lines in Figure 4, parts c and d, is created by unidentified impurities, and translation domain boundaries between (2×1) domains shifted by the single substrate lattice constant (2.95 Å) along the [001] substrate direction. In some cases, the domain boundary contains a kink (see Figure 5a), which can be

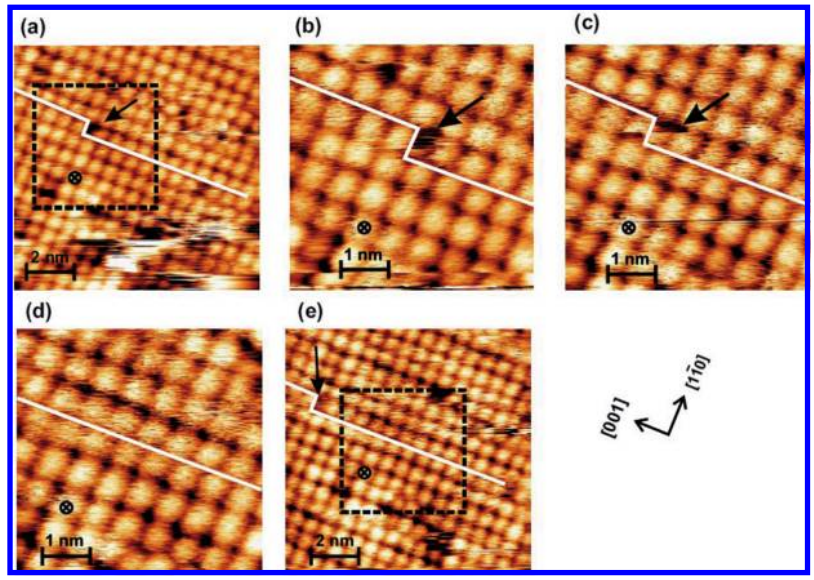

Figure 5. Consecutive STM images showing migration of a single molecule vacation in TPA/TiO_2(110) monolayer. In all images, a crossed circle marks a reference point and the black arrow points to a defect that migrates along the translational domain boundary marked by the white line. The first (a) and last scan (e) present 10 × 10 nm area, whereas scans (b)−(d) show 5 × 5 nm. The area scanned in (b)−(d) scans is marked by black dashed rectangle in scans (a) and (e). All scans were acquired with $I = 2$ pA and $U = 2$ V.

undoubtedly attributed to a molecular vacancy due to spatial limitation. Our STM data show that this single molecular vacancy may move along the domain boundary, as is exemplified by the set of consecutive scans shown in Figure 5. Since observed diffusion was not correlated with the STM scanning direction, we do not attribute it to the tip-induced modification. This observation suggests a rather low barrier for surface diffusion of TPA molecules in the monolayer along the [001] substrate direction.

Exposure Experiment. Considering possible application of TPA monolayers deposited on the TiO_2(110)-(1 × 1) as substrates for MOF structures, the issue of the TPA film stability toward exposure to the air environment becomes crucial. This problem arises because the TiO_2 surface preparation and TPA molecular deposition is accomplished in the UHV system, whereas the MOFs growth process would be performed in the solution consisting of metal ions and organic linkers. To verify the tolerance of the TPA monolayer to the air environment, corresponding sample was removed from the UHV system and kept in air for approximately one hour, and then again reintroduced into the UHV system. Before measurements, the sample was kept in the introduction chamber for several hours without heating to desorb water. The representative STM data recorded for such a sample after air exposure are presented in Figure 6. The results obtained at the molecular resolution level reveal that the molecular film has not suffered severe damage, and practically remained intact contrary to the clean TiO_2 (110) substrate, which is known to be unstable in ambient conditions. Thus, our data justify the possibility of preparing high quality samples of TPA monolayers on TiO_2 substrate in the UHV system, and their later transport through the air environment for further analysis or deposition of other materials. Such a passivation of the TiO_2 surface through an adsorption of pivalate anion was recently used as a method of protection against contamination from the laboratory air in a study of black and ruthenium dyes adsorbed on a rutile TiO_2(110).[18,34]

III. Conclusions

STM measurements of TPA deposited on the rutile TiO_2(110)-(1 × 1) revealed formation of well ordered complete monolayer

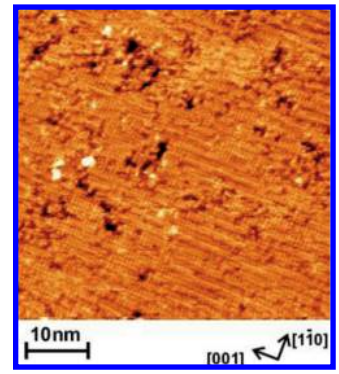

Figure 6. STM image ($I = 2$pA, $U = 2$V) of TPA/TiO_2(110) sample after one hour exposure to the air environment.

at room temperature. The detailed analysis of different STM contrasts, which most probably correspond to imaging different parts of the film's electronic structure, i.e., adsorption sites, molecular backbone, and functional groups, allowed us to propose a model of the TPA adsorption on that surface. In this model, adsorption of the TPA molecules takes place in an upright orientation in the (2 × 1) structure with a rather regular network of dimer rows along the [001] substrate direction. Although the nature of the observed dimerization cannot be fully resolved on the basis of scanning probe techniques only, we propose that dimers are formed as a result of tilting and rotating of neighboring TPA molecules. Our results show that nondestructive STM imaging, enabling proper analysis of the film structure, requires rather high impedance, i.e., low current set point at relatively high bias voltage. This limitation is particularly important for imaging TPA film at the submonolayer coverage and correct identification of the inherent (i.e., not tip induced) defects within the film in the form of missing molecules, domain boundaries and impurities, documented in our studies. The noninvasive STM imaging also allows for direct observation of defects diffusion within the TPA monolayer as exemplified by the detection of the single molecule vacancy migration. Nevertheless, our STM measurements show that these inherent defects do not significantly disturb the order and stability of the TPA monolayer, as it is also demonstrated by

its resistance against exposure to the air environment. The latter property is particularly important since it enables ex situ analysis of this system, and its further treatment in the non-UHV environment.

Acknowledgment. This work was supported by the sixth Framework Program of the European Commission within the Specific Targeted Research Project "Anchoring of metal-organic frameworks, MOFs, to surfaces, SURMOF", Contract No. NMP4-CT-2006-032109. Three of us would like to acknowledge the support received from the Foundation for Polish Science under: Subsidy No. 11/2007 (M.S. and S.G.) and *Homing* fellowship (P.C.).

References and Notes

(1) Diebold, U. *Surf. Sci. Rep.* **2003**, *48*, 53–229.

(2) Satterfield, C. N. *Heterogeneous Catalysis in Industrial Practice*, 2nd ed.; McGraw-Hill: New York, 1991.

(3) Grirrane, A.; Corma, A.; Garcia, H. *Science* **2008**, *322*, 1661–1664.

(4) Li, B.; Zhao, J.; Onda, K.; Jordan, O. K. D.; Yang, J.; Petek, H. *Science* **2006**, *311*, 1436–1440.

(5) Valden, M.; Lai, X.; Goodman, D. W. *Science* **1998**, *281*, 1647–1650.

(6) Lamaka, S. V.; Zheludkevich, M. L.; Yasakau, K. A.; Serra, R.; Poznyak, S. K.; Ferreira, M. G. S. *Prog. Org. Coat.* **2007**, *58*, 127–135.

(7) Hernandez-Alonso, M. D.; Tejedor-Tejedor, I.; Coronado, J. M.; Soria, J.; Anderson, M. A. *Thin Solid Films* **2006**, *502*, 125–131.

(8) Paulios, I.; Spathis, P.; Grigoriadou, A.; Delidou, K.; Tsoumparis, P. *J. Environ. Sci. Health A* **1999**, *34*, 1455–1471.

(9) Sigmund, W.; Yuh, J.; Park, H.; Maneeratana, V.; Pyrgiotakis, G.; Daga, A.; Taylor, J.; Nino, J. C. *J. Am. Ceram. Soc.* **2006**, *89*, 395–407.

(10) Ruiz, A. M.; Cornet, A.; Shimanoe, K.; Morante, J. R.; Yamazoe, N. *Sens. Actuators, B* **2005**, *108*, 34–40.

(11) Wang, G.; Wang, Q.; Lu, W.; Li, J. H. *J. Phys. Chem. B* **2006**, *110*, 22029–22034.

(12) Mor, G. K.; Varghese, O. K.; Paulose, M.; Ong, K. G.; Grimes, C. A. *Thin Solid Films* **2006**, *496*, 42–48.

(13) Guo, Q.; Williams, E. M. *Surf. Sci.* **1999**, *433*−*436*, 322–326.

(14) Schnadt, J.; O'Shea, J. N.; Patthey, L.; Schliessling, J.; Krempasky, J.; Shi, M.; Martensson, N.; Brühwiler, P. A. *Surf. Sci.* **2003**, *544*, 74–86.

(15) Schnadt, J.; Schiessling, J.; O'Shea, J. N.; Gray, S. M.; Patthey, L.; Johansson, M. K. J.; Shi, M.; Krempasky, J.; Ahlund, J.; Karlsson, P. G.; Persson, P.; Martensson, N.; Brühwiler, P. A. *Surf. Sci.* **2003**, *540*, 39–54.

(16) Heanderson, M. A.; White, J. M.; Uetsuka, H.; Onishi, H. *J. Am. Chem. Soc.* **2003**, *125*, 14974–14975.

(17) Qiu, T.; Barteau, M. A. *J. Colloid Interface Sci.* **2006**, *303*, 229–235.

(18) Sasahara, A.; Pang, C. L.; Onishi, H. *J. Phys. Chem. C* **2006**, *110*, 4751–4755.

(19) Palmgren, P.; Yu, S.; Hennies, F.; Nilson, K.; Akermark, B.; Göthelied, M. J. *J. Chem. Phys.* **2008**, *129*, 074707.

(20) Tekiel, A.; Prauzner-Bechcicki, J. S.; Godlewski, S.; Budzioch, J.; Szymonski, M. *J. Phys. Chem. C* **2008**, *112*, 12606–12609.

(21) Yaghi, O. M.; O'Keeffe, M.; Ockwig, N. W.; Chae, H. K.; Eddaoudi, M.; Kim, J. *Nature (London)* **2003**, *423*, 705–714.

(22) Shekhah, O.; Wang, H.; Kowarik, S.; Schreiber, F.; Pauluns, M.; Tolan, M.; Sternemann, C.; Evers, F.; Zacher, D.; Fischer, R. A.; Woll, C. *J. Am. Chem. Sci.* **2007**, *129*, 15118–15119.

(23) Biemmi, E.; Scherb, C.; Bein, T. *J. Am. Chem. Sci.* **2007**, *129*, 8054–8055.

(24) Szelagowska-Kunstman, K.; Cyganik, P.; Goryl, M.; Zacher, D.; Puterova, Z.; Fischer, R. A.; Szymonski, M. *J. Am. Chem. Soc.* **2008**, *130*, 14446–14447.

(25) *SURMOF*,−acronym for the EU-founded STREP type project NMP4-CT-2006−032109.

(26) Allendorf, M. D.; Houk, R. J. T.; Andruszkiewicz, L.; Talin, A. A.; Pikarsky, J.; Choudhury, A.; Gall, K. A.; Hesketh, P. J. *J. Am. Chem. Soc.* **2008**, *130*, 14404–14405.

(27) Horcas, I.; Fernandez, R.; Gomez-Rodriguez, J.; Colchero, J.; Gomez-Herrero, J.; Baro, A. M. *Rev. Sci. Instrum.* **2007**, *78*, 013705.

(28) Lyubinetsky, I.; Yu, Z. Q.; Henderson, M. A. *J. Phys. Chem. C* **2007**, *111*, 4342–4346.

(29) Ito, T.; Bühlmann, P.; Umazewa, Y. *Anal. Chem.* **1998**, *70*, 255–259.

(30) Ito, T.; Bühlmann, P.; Umazewa, Y. *Anal. Chem.* **1999**, *71*, 1699–1705.

(31) Wendt, S.; Schaub, R.; Matthiesen, J.; Vestergaard, E. K.; Wahlström, E.; Rasmussen, M. D.; Thostrup, P.; Molina, L. M.; Leagsgaard, E.; Stensgaard, I.; Hammer, B.; Besenbacher, F. *Surf. Sci.* **2005**, *598*, 226–245.

(32) Atodiresei, N.; Caciuc, V.; Schroeder, K.; Blügel, S. *Phys. Rev. B* **2007**, *76*, 115433.

(33) Watkins, M.; Trevethan, T.; Sushko, M. L.; Shluger, A. *J. Phys. Chem. C* **2008**, *112*, 4226–4231.

(34) Ikeda, M.; Koide, N.; Han, L.; Sasahara, A.; Onishi, H. *Langmuir* **2008**, *24*, 8056–8060.

JP901184T